JOURNAL OF AIRCRAFT
Vol. 46, No. 5, September–October 2009

Three-Degree Decelerating Approaches in High-Density Arrival Streams

A. M. P. de Leege,* A. C. in 't Veld,† M. Mulder,‡ and M. M. van Paassen§
Delft University of Technology, 2629 HS Delft, The Netherlands

DOI: 10.2514/1.42420

Trajectory unpredictability of aircraft performing continuous descent approaches results in reduced runway capacity, because more spacing is applied. A possible solution to this problem is self-spacing: the transfer of the spacing task from the controller to the pilot. Using a fast-time simulation tool, the performance differences between distance- and time-based self-spacing in high-density traffic in terms of runway capacity and separation are quantified for the three-degree decelerating approach. Distance-based self-spacing is the most promising concept. The average runway capacity is 39 aircraft per hour (40% heavy, 60% medium aircraft). Runway capacity in the case of time-based self-spacing is 3 aircraft per hour lower, due to spacing margins applied to lower the separation violation rate to the level of distance-based spacing. A sensitivity analysis was carried out for distance-based self-spacing. One of the results is that accurately determining the starting time and subsequently arriving at this time benefits the three-degree decelerating approach performance. Three-degree decelerating approach performance is also affected by the initial speed and altitude, as they affect the three-degree decelerating approach's control space.

I. Introduction

CONTINUOUS descent approach (CDA) is a cost-effective means of reducing aircraft noise, emissions, flight time, and fuel burn [1–4]. Aircraft continuously decelerate while on these approaches, which leads to trajectory unpredictability from the standpoint of a controller who is monitoring interaircraft spacing based on periodic radar updates of aircraft position. As such, controllers apply larger spacing to prevent vectoring instructions that would conflict with the CDA. Larger spacing between aircraft reduces runway capacity down to 50% when compared with conventional approaches [5–8].

A possible solution to this problem is the use of in-trail self-spacing [6,7]. The spacing task is transferred from the controller to the pilot. Self-spacing is proposed because of the availability of precise aircraft performance information and the control strategy onboard the aircraft. The maneuverability of an aircraft while executing a CDA is limited and driven by the aircraft performance, the control strategy, and wind conditions. Information about wind conditions that the aircraft is likely to encounter during descent can be made available as described in [9]. The flight crew can plan and execute, with the help of onboard systems, a CDA to remain safely separated [10–12].

This paper discusses research into the performance of the three-degree decelerating approach (TDDA) in high-density arrival streams in a distance- or time-based self-spacing environment. The TDDA is a CDA that lies within the boundaries of present approach procedure limitations and gives the pilot control over the descent path to fulfill the spacing task [6,9–13]. In a distance-based self-spacing environment the aircraft actively adapts its speed profile to the speed profile of the aircraft flying directly in front. This requires that the aircraft predicts the trajectory of this leading aircraft. Using the relative state of the leading aircraft to predict the trajectory can give rise to transient motions in the arrival stream, hereafter referred to as the "slinky effect," resulting in spacing problems [14]. In this research, intent-based trajectory prediction is introduced for the TDDA to prevent the slinky effect in the case of distance-based self-spacing. Another solution to circumvent the slinky effect is a time-based self-spacing procedure, which does not require trajectory prediction of the leading aircraft during the TDDA [9]. Its performance was compared with the more common distance-based procedure. In the time-based environment the aircraft receive a required time of arrival (RTA) for the runway threshold point. The RTA are set before the start of the TDDA with the aim to keep the aircraft safely separated during approach. A fast-time simulation tool was developed to investigate the differences in performance between distance- and time-based self-spacing in terms of capacity and loss of separation.

II. Three-Degree Decelerating Approach

A. Description of the Procedure

The TDDA is a straight-in approach, with a constant 3 deg geometrical path angle [13]. Figure 1 illustrates the TDDA together with a conventional step-down approach. The approach procedure starts when the aircraft intercepts the fixed descent path at an altitude (7000–10,000 ft) well above the altitude that the aircraft intercepts the instrument landing system's glide slope. Initially, the aircraft maintains a constant indicated airspeed (IAS).

To perform the spacing task, control over the descent is required. The TDDA gives the pilot two controls. The first control option is the thrust cutback (TCB) altitude, in which engine thrust is set to idle and the aircraft starts to decelerate. Moving the TCB altitude up results in a slower descent and moving the TCB altitude down speeds up the descent. The second control option available after the TCB is flap scheduling. After the TCB, the aircraft starts to decelerate. By changing flaps speeds, the pilot controls the deceleration of the aircraft along the flight path. During the TDDA the pilot performs two tasks. One task is the spacing task in a distance-based or time-based self-spacing environment. The second task is to bring the aircraft in a stabilized landing configuration at the 1000 ft reference altitude h_{ref} at approach speed V_{app} for safety reasons. Below h_{ref}, the aircraft maintains V_{app}. Reaching V_{app} above h_{ref} is not desired

Presented as Paper 7403 at the AIAA Guidance, Navigation and Control Conference and Exhibit, Honolulu, HI, 18–21 August 2008; received 27 November 2008; revision received 6 February 2009; accepted for publication 6 February 2009.

*Ph.D. Student, Faculty of Aerospace Engineering, Kluyverweg 1; arjen.deleege@to70.nl.

†Research Associate, Faculty of Aerospace Engineering, Kluyverweg 1; a.c.intveld@tudelft.nl. Member AIAA.

‡Professor, Faculty of Aerospace Engineering, Kluyverweg 1; m.mulder@tudelft.nl. Member AIAA.

§Associate Professor, Faculty of Aerospace Engineering, Kluyverweg 1; m.m.vanpaassen@tudelft.nl. Member AIAA.

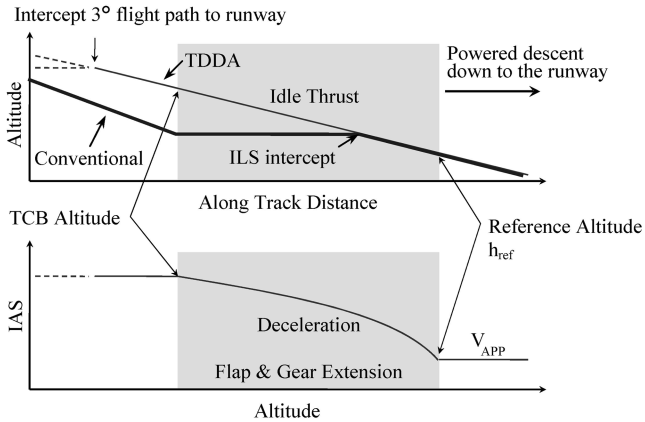

Fig. 1 The three-degree decelerating approach profile.

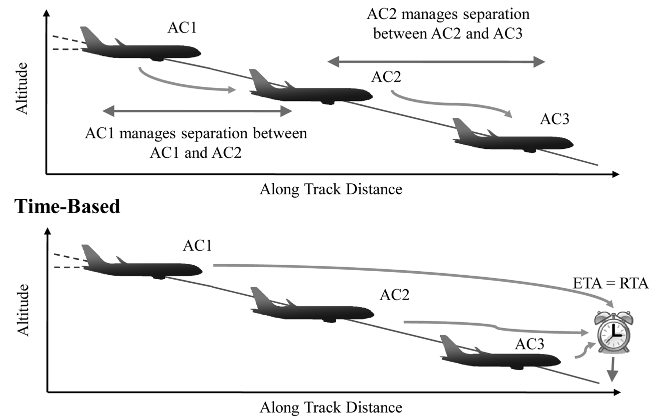

Fig. 2 Time- and distance-based self-spacing compared.

because engine thrust has to be reapplied, negating noise and fuel benefits.

B. Self-Spacing Task

The aim of the self-spacing task is to control the aircraft such that the minimum distance to the leading aircraft equals the minimum safe separation. In this situation, the highest runway capacity is achieved for a fixed sequence. The separation minima used in this research are listed in Table 1. The self-spacing tasks in distance-based and time-based self-spacing environments are different.

1. Distance-Based Self-Spacing

Input for the self-spacing task in distance-based self-spacing is the predicted minimum distance between the own aircraft and the leading aircraft and the separation minimum. If this prediction indicates that the separation minima will be violated, the approach of the own aircraft has to be slowed down such that the minimum distance between the aircraft equals the separation minimum. If necessary, the aircraft may decelerate to V_{app} before reaching h_{ref}. If the predicted minimum exceeds the separation minimum, a faster approach profile should be selected if available. From a safety point of view, no approach should be selected in which V_{app} is reached below h_{ref}, even if this would close the spacing gap between the aircraft. In a distance-based self-spacing environment, the pilot has two performance goals: First, the minimum distance to preceding aircraft should equal the applicable separation minimum, hereafter referred to as the separation goal. Second, the aircraft should reach V_{app} when at h_{ref}, hereafter referred to as the noise goal.

2. Time-Based Self-Spacing

In the time-based self-spacing environment, the aircraft in the arrival stream adhere to a RTA for the runway threshold point. The RTA is computed before the aircraft starts the TDDA and is based on early predictions of the TDDA trajectories of the own aircraft and leading aircraft. The RTA is fixed during the TDDA. The RTA can be provided by the air traffic service provider but could also be calculated onboard the aircraft. Section V describes the methodology used in the simulations to compute the RTA. In the time-based concept, the pilot has two performance goals: first is to cross the runway threshold at the RTA (time goal) and second is the noise goal that is also applied in the distance-based environment. Figure 2 compares the self-spacing concepts.

Table 1 Separation minima in nautical miles, by weight category

	Trailing aircraft		
Leading aircraft	Heavy	Medium	Light
Heavy	4	5	6
Medium	4	4	5
Light	2.5	2.5	2.5

3. TDDA Pilot Support Algorithms

Previous research showed that it is difficult for pilots to determine the correct TCB altitude and flap schedule [10,11]. Therefore, the pilot is supported by TCB altitude and flap scheduling optimization algorithms fed by wind and trajectory predictions to meet the noise goal and separation or time goal [9–11]. Figure 3 gives an overview of the algorithms used to provide the pilot with a TCB altitude and flap schedule in the distance-based self-spacing environment. Shown on the left are the three algorithms that provide the input for the TCB altitude, and flap schedule optimization algorithms are on the right. The wind prediction algorithm used in this research is the advanced wind prediction algorithm described in [9]. The output is a wind profile that the aircraft is likely to encounter during descent. The algorithm is driven by automated meteorological data relay (AMDAR) observations received from aircraft in the vicinity. The observations are stored, ordered, and filtered to obtain a wind prediction. Trajectory prediction of the own aircraft uses an onboard performance model. Inputs are the current state of the aircraft, planned TCB altitude, flap schedule, and wind prediction. Trajectory prediction of the leading aircraft uses an aircraft intent-based prediction model that is addressed in Sec. III. In addition to an aircraft intent description of the leading aircraft, the wind prediction is used. From the trajectory predictions, the minimum distance between the aircraft is derived.

The minimum distance is compared with the separation goal (the separation minimum). The trajectory prediction of own the aircraft is also used to determine the altitude at which V_{app} is reached to check against the noise goal. When the aircraft position is still above the last computed TCB altitude, TCB optimization continues until all performance goals are met. The separation goal has priority over the noise goal when the minimum separation between the aircraft is less than the separation minimum. The noise goal has priority over the separation goal when the minimum separation between the aircraft exceeds the separation minimum. Once below the TCB altitude, flap schedule optimization is started. The flap scheduler is based on the scheduler developed by de Prins et al. [10]. The flap scheduler uses a binary search algorithm to determine the optimal schedule. The scheduler only optimizes for the noise goal if the separation goal is met, thus giving priority to the separation task.

The TDDA algorithm structure for time-based self-spacing is similar to the structure used for distance-based spacing (see Fig. 4). The minimum distance between the aircraft is no longer computed and is replaced by the estimated time of arrival (ETA), which is checked against the RTA. In the TCB altitude and flap schedule optimization algorithms, the time goal is treated in a similar way as the separation goal.

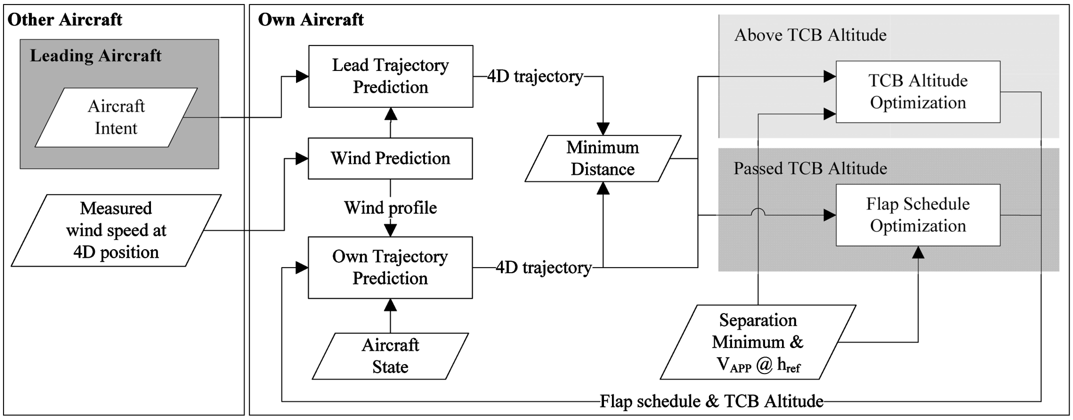

Fig. 3 Structure of TDDA algorithm for distance-based self-spacing.

III. Aircraft Intent-Based Trajectory Prediction

To prevent the slinky effect during distance-based self-spacing, aircraft intent is used to predict the trajectory of the leading aircraft. Captured in the intent is the outcome of optimization of the trajectory by the TDDA algorithms onboard the leading aircraft. If an aircraft descent profile is disturbed (for instance, by a wind change or delayed pilot action), the TDDA algorithm optimizes the trajectory. The new trajectory is described in aircraft intent that may be different from the previous intent information, because of the optimization process. The intent is exchanged using a data link. Predictions based only on previous states do not account for the ongoing optimization process. This can cause unnecessary control actions from the trailing aircraft that can propagate through the arrival stream, resulting in the slinky effect.

A. Aircraft Intent Description of the TDDA

Aircraft intent is an unambiguous description of how the aircraft is to be operated within a time frame. The intent information is the input to a trajectory predictor [15]. The TDDA procedure can be expressed in terms of aircraft intent and consists of three segments: descent along the glide slope with constant IAS down to the TCB altitude; descent and deceleration along the glide slope down to the altitude at which V_{app} is reached, normally 1000 ft above the runway (during this segment the flaps and landing gear are extended); and descent along the glide slope with constant IAS (V_{app}) down to the runway threshold.

Before continuing with the design of the trajectory predictor based on aircraft intent, the relevance of the leading aircraft prediction has to be analyzed.

B. Point of Minimum Separation

When the relative ground speed of the trailing aircraft is higher than the leading aircraft, the separation reduces. For two aircraft on CDA, this is generally the case, and minimum separation takes place when the leading aircraft passes the runway threshold. One exception is when the leading aircraft is locked into its own approach speed while the trailing aircraft is still decelerating to meet its approach speed and the ground speed of the trailing aircraft has dropped below the leading aircraft. A headwind component that increases with altitude can have the same effect. Simulations of arrival streams of aircraft performing a TDDA under actual wind conditions indicated that the minimum separation takes places when the leading aircraft has passed h_{ref} and maintains a constant IAS [16].

C. Intent-Based Trajectory Prediction

A prediction of the last constant speed segment is sufficient to determine the minimum separation. This segment can be predicted independent of the other segments using the leading aircraft ETA, V_{app}, and flight-path angle as illustrated in Fig. 5.

The speed and flight-path angle are constant during the last stage of the final approach. Only aircraft intent information is needed for the prediction. The predictor starts at the runway threshold at which the aircraft is at the ETA with speed V_{app} and computes the trajectory up to the reference altitude. Because the aircraft maintains a constant IAS, no aerodynamic performance model of the leading aircraft is required. A wind prediction is supplied by the wind predictor.

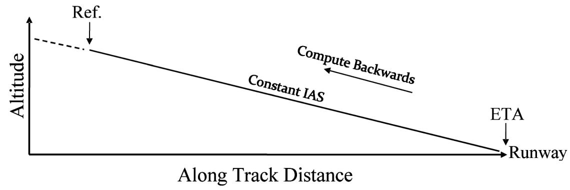

Fig. 5 Intent-based trajectory prediction.

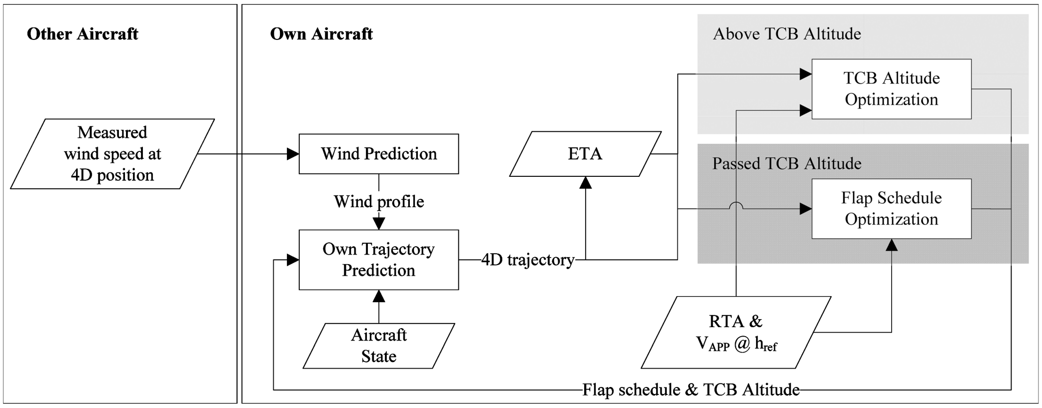

Fig. 4 Structure of TDDA algorithm for time-based self-spacing.

IV. TDDAs in Arrival Streams

An arrival stream consists of aircraft aligned to land on the same runway. The aircraft in the stream vary in type and weight and have different aircraft performance characteristics. This imposes constraints on the initial separation between aircraft at the start of the TDDA. These constraints are determined by the size of the TDDA control space and the separation minimum or RTA. The control space is defined as the time interval between the earliest and latest possible arrivals for a given starting time.

A. Factors that Affect the TDDA Control Space

The boundaries of the TDDA's control space are a function of the aircraft type, weight, and wind conditions. Figure 6 gives the control spaces under three wind conditions for a medium-range aircraft. The boundaries are the TDDAs with the shortest and longest durations. To get the shortest duration, all flaps are extended at their maximum speed, resulting in a fast but late deceleration and the lowest possible TCB altitude. The longest duration is achieved by extending flaps at their minimum speed, resulting in a gradual and early deceleration and the highest possible TCB altitude.

From Fig. 6, the minimum and maximum time-to-fly can be derived. Alternatively, the control space can be expressed in terms of the TCB altitude, as shown in Fig. 7. The figure shows the range of TCB altitudes for which the noise goal can be met. A headwind increases the duration of the TDDA and lowers the TCB altitudes, but also makes the control space smaller. A tailwind has the opposite effect.

B. Effect of Initial Separation on TDDA

Figure 8 shows a TDDA control space for three different initial separations behind a leading aircraft in a distance-based self-spacing environment. The separation goal is visualized by offsetting the leading aircraft trajectory prediction over the required separation away from the runway (separation boundary). The separation boundary gives the minimum allowable distance to the runway threshold.

For the upper control space, the initial separation is too small. The separation boundary crosses the full control space. The aircraft must reduce speed to V_{app} before the aircraft passes h_{ref}; otherwise, there will be a loss of separation. If the separation boundary does not cross the control space, which is the case for the lower control space, there will be a spacing gap with a negative effect on the runway capacity. The aircraft is not able to fly the TDDA fast enough to close this gap.

Only when the separation boundary ends in the control space is a TDDA possible that meets the performance goals. Figures 9 and 10 show two possible trajectories for TDDAs with the highest and lowest possible TCBs that meet the performance goals. A high TCB altitude is preferred because of the positive effect on the aircraft noise and fuel use and because of less flap wear. For time-based self-spacing, the separation is replaced by the RTA.

C. Initial Separation Constraints: Distance-Based Self-Spacing

Using the control-space and separation boundaries, the initial separation constraints can be determined. Figure 11 illustrates how

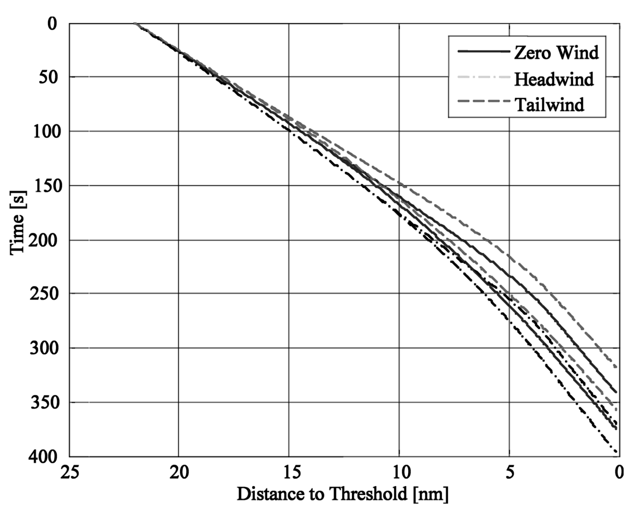

Fig. 6 Control space time vs distance for three wind conditions.

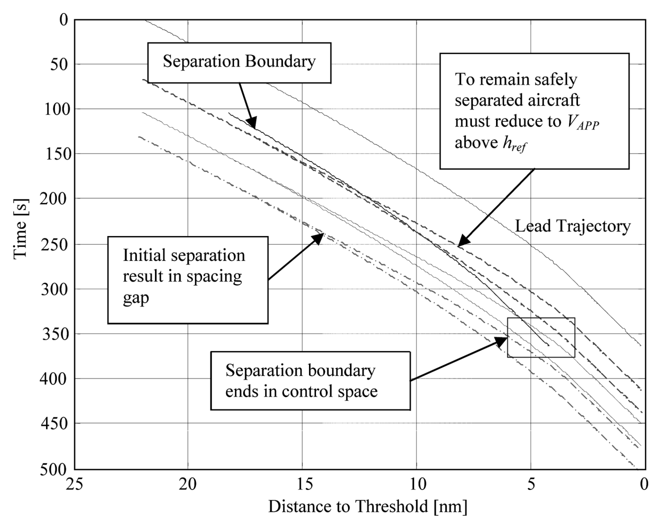

Fig. 8 Effect of initial separation on TDDA performance.

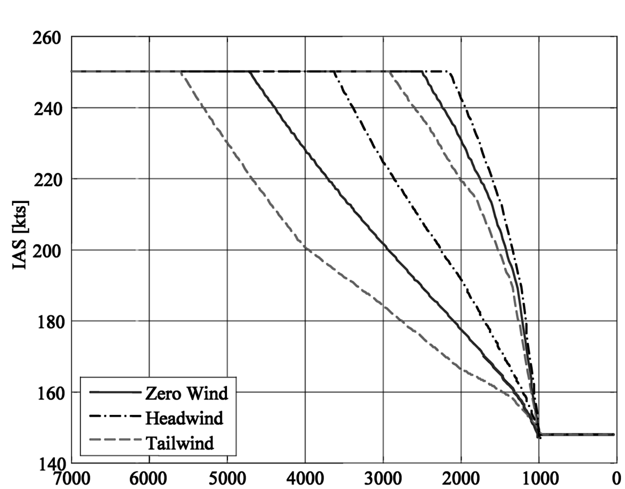

Fig. 7 Control space IAS vs altitude for three wind conditions.

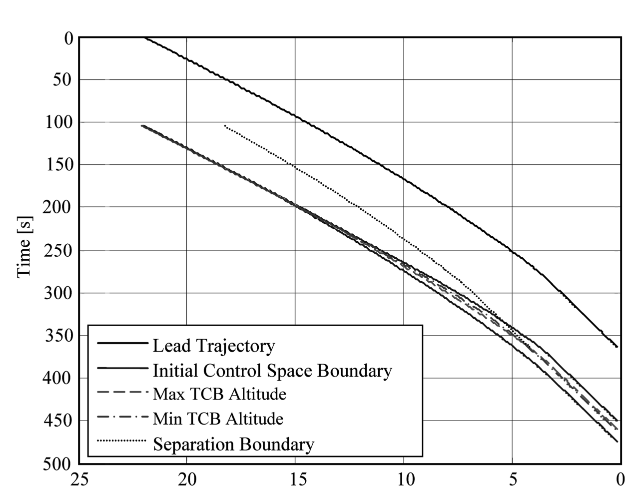

Fig. 9 Feasible TDDA trajectories.

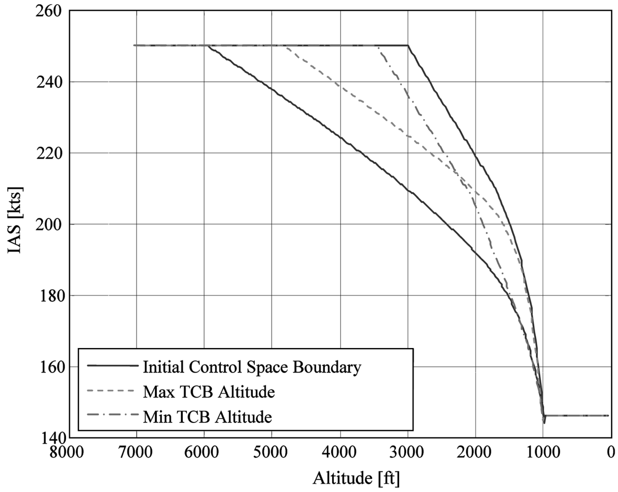

Fig. 10 Feasible TCB altitudes.

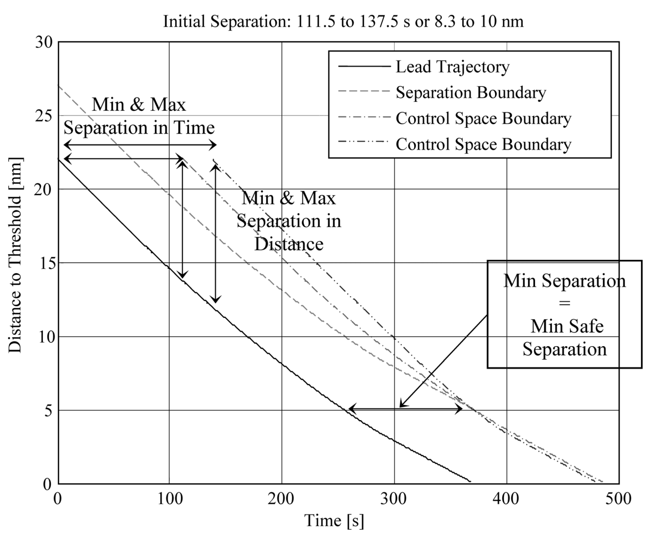

Fig. 11 Minimum and maximum initial separation for distance-based spacing.

these constraints are determined for distance-based self-spacing. The control-space boundaries are positioned such that the minimum separation equals the minimum safe separation; hence, the minimum and maximum initial separations are visible.

D. Initial Separation Constraints: Time-Based Self-Spacing

The initial separation constraints in the case of time-based spacing are determined in a similar way. The arrival time of the control-space boundaries is set equal to the RTA from which the entry time interval is determined (see Fig. 12). For the sake of reference, the separation boundary is drawn; hence, the minimum separation between the aircraft should not be violated.

V. Fast-Time TDDA Simulation Tool

The fast-time simulation tool simulates arrival streams of aircraft executing the TDDA in a distance- or time-based self-spacing environment under actual wind conditions. Implemented in the simulator is the TDDA with the optimization and scheduling algorithms depicted in Figs. 3 and 4.

A. Aircraft Model

For the aircraft trajectory simulation and trajectory prediction, point-mass models are used that approximate the following aircraft:

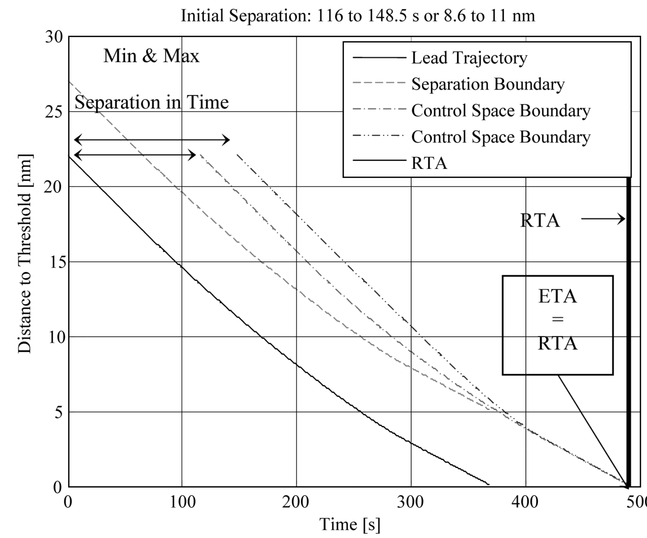

Fig. 12 Minimum and maximum initial separation for time-based spacing.

Boeing 747-400, 777-300, 737-400, and 737-800 and the Airbus 321. The models resemble the performance differences between different aircraft types and sizes, which is more important for this research than a very precise modeling of the aircraft performance. The equations of motion are derived using Figs. 13 and 14.

For small angles of attack α and assuming that the geometric-path angle equals the aerodynamic-path angle ($\gamma_k = \gamma_a$), the equations of motion in the kinematic reference frame F_k along the fixed flight path are

$$\sum F_Z\colon\ 0 = L - mg\cos\gamma_k \tag{1}$$

$$\sum F_X\colon\ m\ddot{x}_k = T - D + mg\sin\gamma_k \tag{2}$$

The mass is assumed to remain constant during the simulation and is used to determine the required lift force L and drag D. Subsequently, the aerodynamic coefficients C_L and C_D and thrust are computed. The approach speed V_{app} is 1.3 times the stall speed in the landing configuration plus 10 kt. Maximum flap extension speeds are obtained from the aircraft manufacturer or operator. Minimum speed for an aircraft configuration is 1.3 times the stall speed for that configuration.

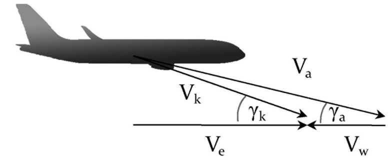

Fig. 13 Kinetic diagram.

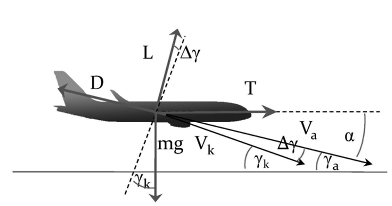

Fig. 14 Force diagram.

B. Pilot Response Time and Wind

The pilot response time for flap and gear deployment is modeled using the pilot response delay model described in [5]. The model consists of a normal distribution fitted to pilot response time data collected during an experiment to investigate the variables that influence the performance of noise abatement procedures. AMDAR observations have been used to create 54 time-varying wind profiles of approximately 1 h. For simulation of the aircraft trajectory, the observations are used. For the wind prediction algorithm, noise is superimposed on the observations to simulate measurement errors.

C. Setting the RTA and Initial Separation

The RTA and starting time for an aircraft are set 600 s before the leading aircraft starts the TDDA. Use is made of the prediction algorithms described in Sec. II to compute the control-space boundaries and initial separation constraints. A 0.2 n mile buffer is added to the separation minima to account for uncertainties in the predictions (wind changes). The size of the buffer was determined using trial and error. To set the RTA, the procedure to determine the initial separation constraints for distance-based self-spacing is followed. The RTA is set to the latest crossing of the control-space boundaries with the time axis to account for trajectory deviations. The starting times position the aircraft exactly between the initial separation constraints.

VI. Distance- and Time-Based Self-Spacing Performance

Using the simulation tool, 5000 arrival streams consisting of eight aircraft have been simulated for both self-spacing environments. The aircraft type was selected randomly from the five available aircraft models. Per aircraft type, three different weights were assigned randomly to the aircraft: the operating empty weight, the maximum landing weight, and the mean of the operating empty weight and maximum landing weight. The TDDA starts at 7000 ft with 230 kt IAS. The performance of the TDDA in high-traffic-density arrival streams in the two self-spacing environments was assessed using the formulated noise, separation, time goal, and runway capacity.

A. Noise Goal

The noise goal is met if V_{app} is reached at h_{ref}. Figure 15 shows the average altitude at which V_{app} was reached, hereafter referred to as $h_{V_{\text{app}}}$, per position in the arrival stream. As expected for time-based self-spacing, no trend between the position of the aircraft and $h_{V_{\text{app}}}$ could be identified ($R = 0.006$ and $p = 0.287$ for a Pearson 2-tailed). On average, $h_{V_{\text{app}}}$ lies 20 ft above h_{ref}. When taking tolerances used by algorithms into account, it is concluded that, on average, the noise goal is met. For the distance-based scenario, a positive correlation between $h_{V_{\text{app}}}$ and the position in the stream can be identified ($R = 0.145$ and $p < 0.001$ for a Pearson 2-tailed). The noise reduction deteriorates toward the end of the arrival stream. From the median and 5th to 95th percentiles, it can be concluded that the number of aircraft that fail the noise goal remains almost constant, but that the deviation from h_{ref} increases (see Fig. 16).

Deterioration of the noise reduction is caused by accumulation of delays (slowdown effect) in the arrival stream. If there is delay in the arrival stream, all trailing aircraft in the stream are affected by this delay. Aircraft in the end of arrival stream are confronted with longer delays than the aircraft in the beginning of the arrival stream. To remain safely separated, aircraft increase the TCB altitude to the upper bound of their control space. If this is not sufficient, flap extension is advanced, but this will result in failure to meet the noise goal. In the case of a delayed arrival, there is a significant correlation between h_{ref} and the magnitude of the delay ($R = 0.672$ and $p < 0.001$ for a Pearson 2-tailed). When an aircraft arrives earlier than initially planned, no effect on the noise goal can be identified ($R = 0.057$ and $p < 0.001$ for a Pearson 2-tailed).

Deterioration of the noise reduction due to accumulating time delays was suppressed by increasing the initial separation between the aircraft in the end of the arrival stream. The 0.2 n mile buffer was increased for the last four aircraft to 0.5 n mile. The aircraft first use the additional spacing when confronted with a delay before starting to move the TCB. The result is that the aircraft still reach V_{app} at h_{ref} (see Fig. 17). A positive correlation between $h_{V_{\text{app}}}$ and the position cannot be identified ($R = 0.040$ and $p < 0.001$ for a Pearson 2-tailed).

B. Separation

Table 2 shows the deviation of the RTA for time-based self-spacing. All aircraft arrived within 49.5 s from the RTA and 99% of the aircraft arrived within 6.5 s of the RTA. The two self-spacing concepts are compared using the separation margin. The separation margin is defined as the actual minimum separation minus the minimum allowable separation; hence, a positive margin yields a spacing gap and a negative margin yields a separation loss. Visible in the histograms in Fig. 18 are the 0.2 n mile buffer applied in the case of time-based self-spacing and the 0.2 and 0.5 n mile buffers for the distance-based scenario. In both self-spacing environments, separation violations do occur (see Table 3). Under distance-based self-spacing, there was a separation loss between 0.32% of the aircraft pairs. This percentage is comparable with go-around percentages reported by two major U.K. airports: London Heathrow had 0.24% and London Gatwick had 0.31% of the total annual arrivals [17,18]. At this stage of the research, this is deemed to be an acceptable reference level. Furthermore, other possible measures to

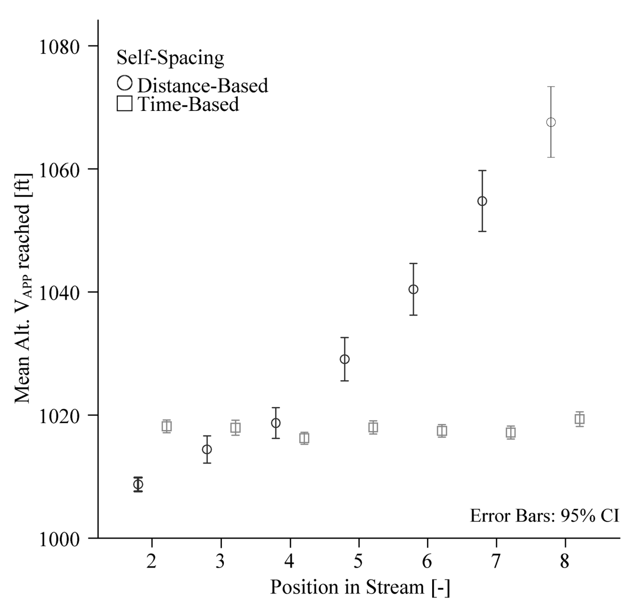

Fig. 15 Altitude V_{app} reached.

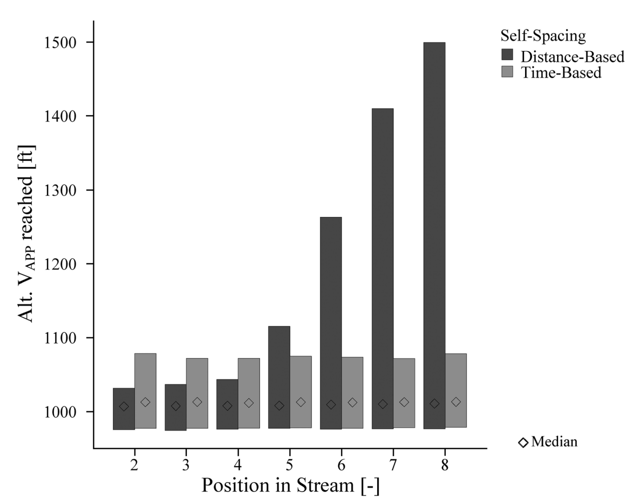

Fig. 16 Median and 5th to 95th percentile of altitude V_{app} reached.

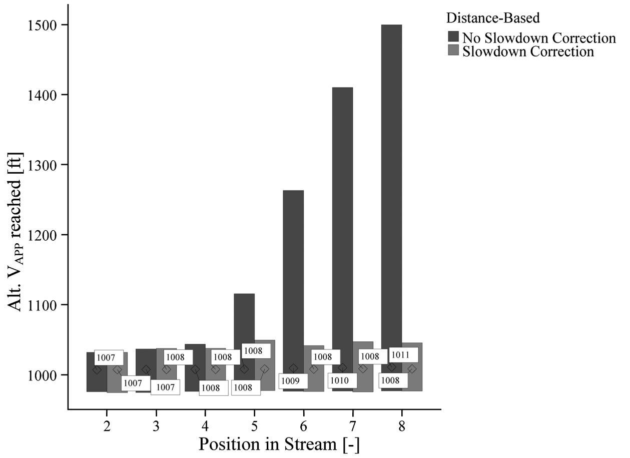

Fig. 17 Effect of slowdown correction on median and 5th to 95th percentile of altitude V_{app}.

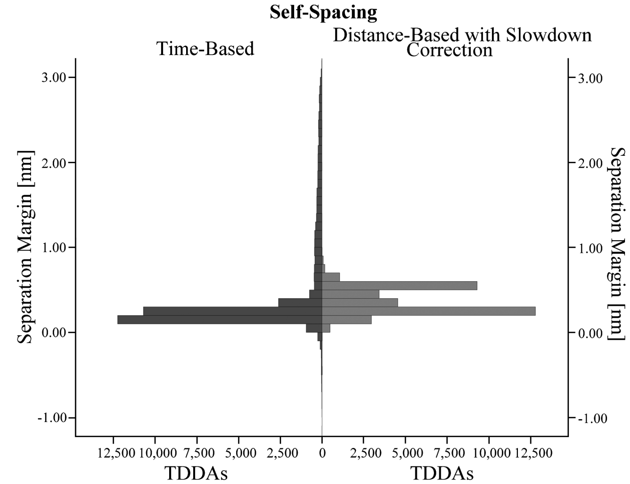

Fig. 18 Separation margin.

bring this percentage down (e.g., the use of speed brakes) have not been evaluated because of limitations of the fast-time simulator.

In the case of time-based self-spacing, the separation violation percentage is 1.42%. To lower the violation rate for time-based spacing to the level of distance-based spacing, the separation buffer was extended by 0.3 to 0.5 n mile. As a result, the separation violation percentage dropped to 0.27% and the separation margin increased (see Table 3).

C. Capacity

For evaluation of the runway capacity, the time-based scenario with the extended separation buffer is used, such that the separation violation percentage is similar. For the distance-based self-spacing, use is made of the arrival stream initially described in Sec. VI with the slowdown correction. The capacity figures are based on 5000 randomly created arrival streams per self-spacing concept. Figure 19 shows the histograms of the capacity expressed in aircraft per hour (AC/h) for both forms of self-spacing. Independent of the self-spacing concept, there is some spread in the runway capacity; because the traffic mix (on average, 40% heavy and 60% large) is determined randomly, variation in the runway capacity can be expected.

Use of distance-based spacing results in a higher runway capacity than time-based spacing, as expected due to the 0.5 n mile separation buffer used for time-based spacing. For distance-based self-spacing, the separation buffer was also extended to 0.5 n mile, but only for the last four aircraft. Furthermore, this buffer is used to absorb delays. For the time-based scenario, the average runway capacity is 35.7 aircraft per hour ($\sigma = 3.3$ AC/h); when using distance-based spacing for eight aircraft in the arrival stream, the average capacity is 39.2 aircraft per hour ($\sigma = 3.6$ AC/h). More descriptive statistics are summarized in Table 4. To determine the significance of the difference in runway capacity, an analysis of variance test (ANOVA) is used ($F = 2560.04$ and $p < 0.001$).

A simulation tool for arrival streams executing a conventional approach is not available; this makes an exact capacity comparison impossible. The runway-capacity figures are analyzed using a packing factor. The packing factor PF is defined as

$$\mathrm{PF} = \frac{\sum_{i=2}^{k} S_{\mathrm{allowed}}}{\sum_{i=2}^{k} S_{\mathrm{actual}}} \quad \forall\ S_{\mathrm{actual}} \geq S_{\mathrm{allowed}} \tag{3}$$

where k is the number of the aircraft in the arrival stream, S_{actual} is the actual separation minimum between two aircraft, and S_{allowed} is the minimum safe separation. Separation violations are not included in the PF calculation. If $\mathrm{PF} = 1$, the runway capacity equals the theoretical maximum. As expected from results discussed earlier, the PF for distance-based spacing is higher than for time-based spacing: 0.90 and 0.81, respectively. Both self-spacing scenarios increase runway capacity significantly when compared with runway-capacity figures for current CDA operations [4,6].

Using conventional approach procedures, the PF will also be less than 1. The runway capacity observed in the distance-based simulations is a least 90% of the runway capacity when using conventional approach procedures.

VII. Sensitivity Analysis

Time-based and distance-based self-spacing perform comparably except for the runway capacity, in which the distance-based scenario has a 3 AC/h advantage. Runway capacity is one of the major issues with CDAs in high-density traffic; in that respect, distance-based self-spacing is the most promising option. Therefore, a sensitivity analysis was carried out for the distance-based self-spacing scenario with the slowdown correction. The goal of this study was to investigate the effects of air traffic management performance, top of descent altitude, predictions based on erroneous weight information, and initial speed on the TDDA performance. The main effects are described; possible interactions are the subject of ongoing research.

A. Initial Control Space Prediction

In the simulations, the starting time of the TDDA for an aircraft was set 600 s before the preceding aircraft starts the TDDA, to give the controller and the aircraft sufficient time to let the aircraft arrive at the computed entry time. The required time is the subject of ongoing research. To assess the effect of this time period (lead time to start) on the TDDA performance, the lead time to start is reduced to 0 s in 3 equal steps of 200 s. In case the lead time to start is 0 s, the control

Table 2 Absolute deviation from the RTA in percentiles

Percentile	Deviation, s
1	0.0
25	0.0
50	0.5
75	1.0
99	6.5
100	49.5

Table 3 Separation violations compared

Self-spacing	Mean, n mile	Median, n mile	Separation violations, %
Time-based	0.47	0.22	1.42
Distance-based	0.37	0.31	0.32
Time-based (0.5 n mile buffer)	0.76	0.52	0.27

Table 4 Capacity descriptive statistics in AC/h

Self-spacing	Mean	Median	Std.	Min	Max	Range
Time-based	35.7	35.3	3.3	26.7	49.7	23
Distance-based	39.2	38.8	3.6	30.9	53.3	22.3

space used to determine the starting times for the trailing aircraft are computed when the leading aircraft start the TDDA.

From Fig. 20, it is concluded that the lead time to start affects the TDDA noise-goal performance and TCB altitude, especially those of the last four aircraft in the arrival stream. The noise-goal performance and TCB altitude become less dependent on the position of the aircraft in the arrival stream. The predictions over a shorter time horizon benefit the performance of the TDDA. The number of separation violations and the runway capacity (39.1 AC/h $\pm$ 0.1 and PF $= 0.90$) are not affected.

The slowdown effect is not visible when the lead time to entry is 0 s; hence, the correction is no longer needed. Without the slowdown correction, the capacity would increase to 40.6 AC/h (0.34% separation violations) and only a 5 ft deterioration of the noise goal would be visible. Time-based spacing is still being outperformed by distance-based spacing in case the shortest time period would be feasible, both in terms of capacity (-2.4 AC/h) and separation violations ($+1.38\%$).

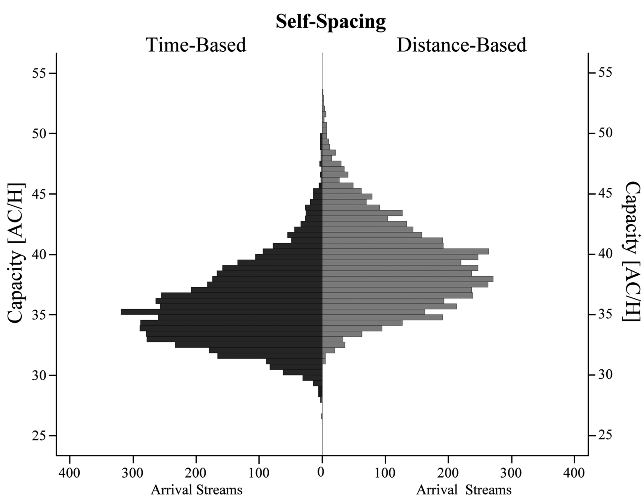

Fig. 19 Runway capacity.

B. Initial Separation Distribution

In the previous sets of simulations, the TDDA starting time was such that the aircraft were positioned in the middle of their control space. It is expected that, in reality, a distribution will be observed around the computed starting time. A new set of simulations was made in which the aircraft were initially positioned around the computed starting time using a normal distribution with the standard deviations σ ranging from 1 to 6 s.

1. *Noise Goal*

Figure 21 shows the median and 5th to 95th percentile of $h_{V_{\mathrm{app}}}$ per position for each initial separation distribution. The noise reduction deteriorates with the increase of the standard deviation σ, but the impact is limited when the standard deviation is below or equal to 3 s. The 3 s standard deviation means that 95% of the aircraft are positioned within 6 s of the middle of the control space, creating a 12 s interval. This interval is equivalent to the smaller control spaces. A bigger standard deviation causes aircraft to be positioned outside the initial separation constrains, making it impossible to fly a TDDA and remain safely separated, as shown in Fig. 8. Because of the additional initial separation applied in the end of the arrival stream, the effect is less strong there.

2. *Separation Violations and Capacity*

The separation violation percentage increases almost exponentially with the standard deviation (see Fig. 22). No significant effect on the runway capacity could be identified ($F = 1.859$ and $p = 0.084$).

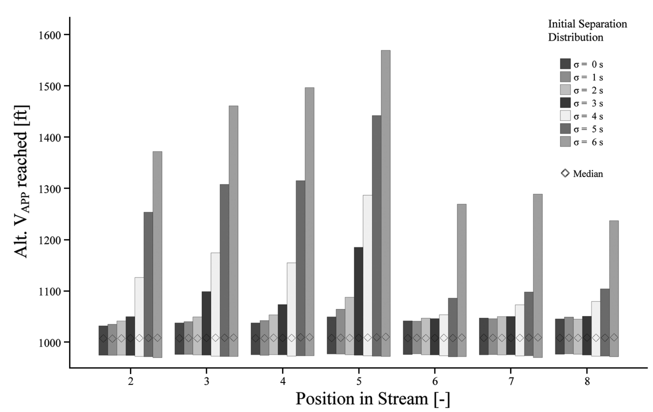

Fig. 21 Median and 5th to 95th percentile of altitude V_{app}.

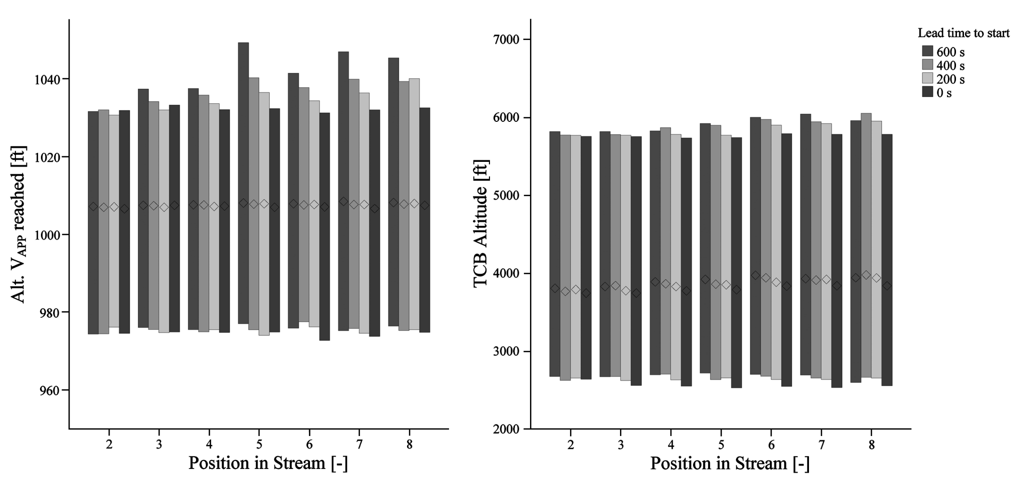

Fig. 20 Median and 5th to 95th percentile of a) altitude V_{app} and b) TCB altitude.

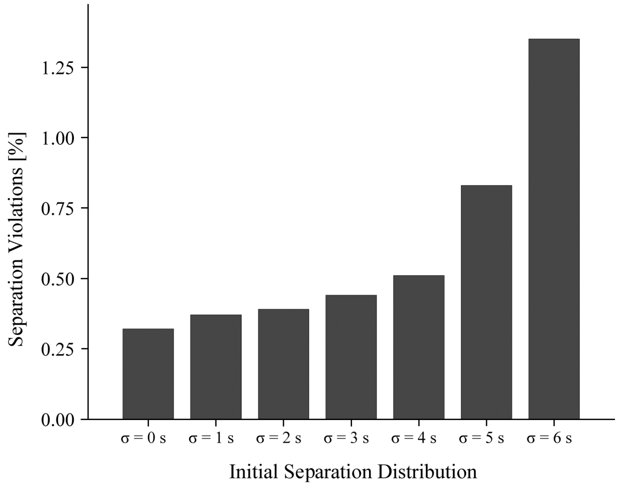

Fig. 22 Effect of initial separation on separation violations.

3. Thrust Cutback Altitude

The initial separation distribution affects the TCB altitude. This is logical, because TCB altitude is related to the control space and initial separation. The mean of the TCB altitude shows a negative trend. The TCB altitude lies approximately 100 ft lower for $\sigma = 6$ s when compared with $\sigma = 0$ s. An ANOVA confirms the effect of the initial separation on the TCB altitude ($F = 9.847$ and $p < 0.001$). The effect depends on the position of the aircraft in the stream ($F = 104.548$ and $p < 0.001$).

C. Starting Altitude

The starting altitude of the TDDA procedure sets the length of the TDDA and the maximum achievable TCB altitude. A higher altitude allows for higher TCB altitudes (see Fig. 23b). The median of TCB altitude increases slightly. The increase of the 95th percentile indicates that only a number of flights with a TCB altitude above the median benefit from the increased starting altitude. The median altitude at which V_{app} is reached remains constant, but the 95th percentile increases, indicating that the deviations from the reference altitude become bigger. A higher starting altitude and thus a longer TDDA lead to an increase of the number separation violations (see Table 5).

D. Initial Speed

Figure 24 shows the effect of the initial speed on the noise-goal performance and the TCB altitude. A lower speed results in a lower TCB altitude but also shrinks the control space. The smaller control space limits the aircraft in their power to account for the slowdown effect. A speed of 230 kt IAS is the maximum possible speed; beyond 230 kt, the acceleration along the glide path cannot be stopped for all aircraft types, due to flap limits (speed brakes are not included in the simulation).

No effect on the runway capacity was expected, because the approach speeds were unchanged; this is confirmed by an ANOVA

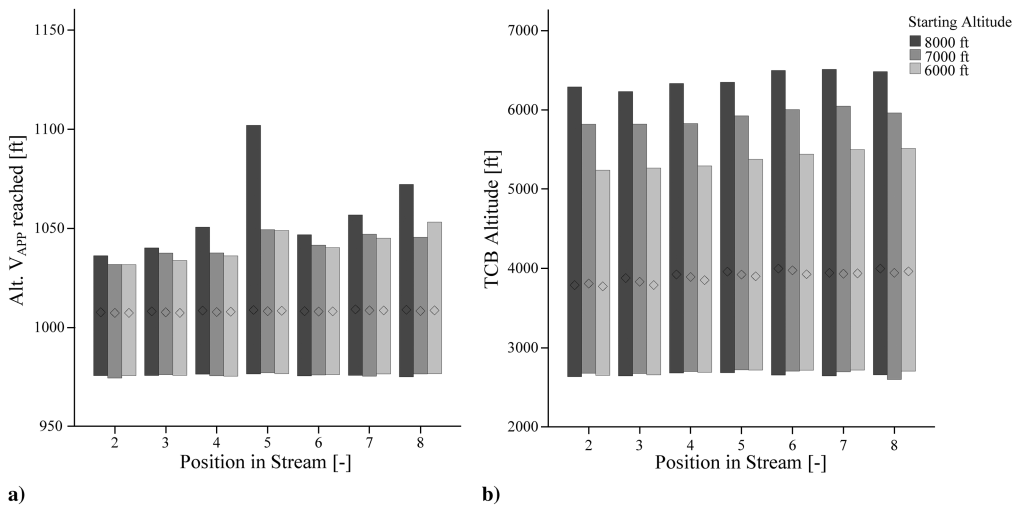

Fig. 23 Effect on the starting altitude on the median and 5th to 95th percentile of a) altitude V_{app} and b) TCB altitude.

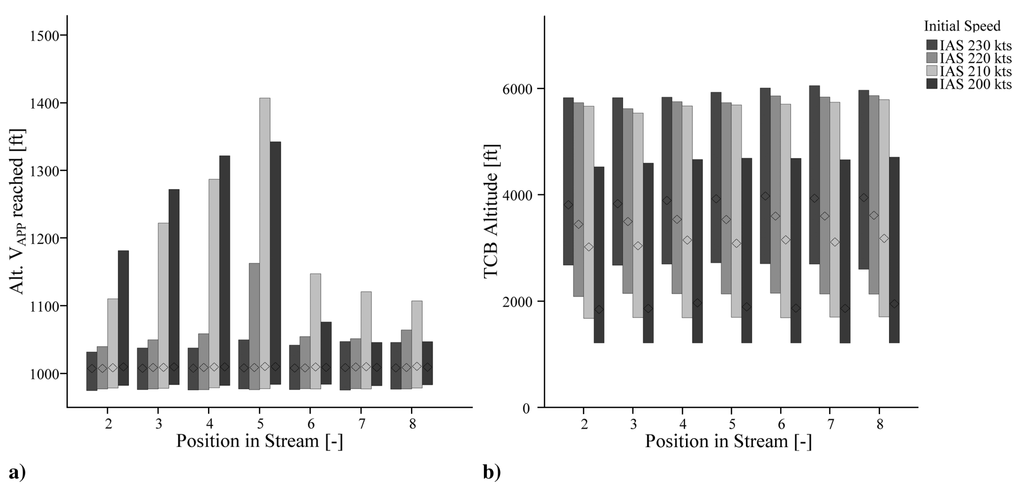

Fig. 24 Effect of the initial speed on the median and 5th to 95th percentile of a) altitude V_{app} and b) TCB altitude.

Table 5 Effect of starting altitude on percent of arrivals with separation violation

Starting altitude, ft	Separation violations, %
8000	0.48
7000	0.32
6000	0.26

Table 6 Effect of initial speed on separation violations

Initial speed, kt	Separation violations, %
230	0.32
220	0.53
210	1.26
200	2.00

($F = 0.627$ and $p < 0.645$). The lower IAS has a negative effect on the control space of the aircraft, with a negative effect on the number of separation violations (see Table 6).

E. Aircraft Weight

The aircraft weight is one of the factors that determines the aircraft performance. In the simulations performed thus far, it was assumed that the weight of the aircraft used by the TDDA algorithms equals the actual weight of the aircraft. Because of the use of standard passenger and baggage weights, it is expected that the computed weight and the actual weight differ. To investigate the effect of differences between the computed and actual weight on the TDDA performance, an error as percentage of the payload was introduced. Three simulations were set up with payload errors up to 0, ± 5, and $\pm 10\%$. The actual percentage per aircraft in the arrival stream was selected using a uniform distribution. No significant effects on the TDDA performance could be identified.

VIII. Discussion

The aim of this research was to evaluate the performance of the TDDA in high-density-traffic arrival streams in a distance- and time-based self-spacing environment. Distance-based self-spacing concepts may suffer from instability of arrival streams, if predictions of the leading aircraft trajectory are based on previous aircraft states. In this research, prediction of the leading aircraft trajectory solely based on intent was introduced in the TDDA. No signs of the slinky effect have been found in the simulated arrival streams. In the case of time-based spacing, the trailing aircraft trajectory is not adjusted as a reaction to changes in the leading aircraft trajectory; hence, the slinky effect is, by definition, not possible.

Application of the TDDA in arrival streams imposes constraints on the initial separation between aircraft. The initial separation interval expressed in time or distance follows from the control space, which is a function of the aircraft type and weight, and the wind conditions.

Under distance-based self-spacing, there was a separation loss between 0.32% of the aircraft pairs. To lower the violation rate for time-based spacing to the level of distance-based spacing, the separation buffer to set the RTA was extended by 0.3 to 0.5 n mile.

For the time-based scenario, the average runway capacity is 35.7 AC/h; when using distance-based spacing, the average capacity is 39.2 AC/h. The runway capacity under distance-based self-spacing is 90% of the theoretical maximum capacity. Because distance-based self-spacing outperformed time-based self-spacing in terms of runway capacity, distance-based self-spacing is considered to be the most promising option.

To further evaluate the performance of the TDDA in a distance-based self-spacing environment, a sensitivity study was carried out. Reducing the time between computing the TDDA starting time and the actual starting time improves the performance of the TDDA. However, this also gives the pilot and controller less time to take actions to let the TDDA start on time. The sensitivity analysis also shows that it is crucial for the aircraft to start the TDDA at the set starting time. When aircraft are positioned outside their control space, the performance degrades. The initial conditions of the TDDA affect the performance. A higher initial speed results in a larger control space, which benefits performance. A higher starting altitude results in higher TCB altitudes but also increases the number separation violations. The trajectory becomes longer, which increases the uncertainties. Trajectory predictions based on erroneous aircraft weight with errors up to 10% of the payload did not have a significant effect on the performance.

IX. Conclusions

Distance-based self-spacing has a 3 AC/h runway-capacity advantage over time-based self-spacing when the number of separation violations between aircraft is comparable. Runway capacity is one of the major factors limiting the use CDAs; in that respect, distance-based self-spacing is the most promising option. The observed runway capacity is 90% of the theoretical maximum. A sensitivity analysis for distance-based self-spacing showed that accurately determining the starting time and the ability to arrive at the starting time with great precision benefits the TDDA performance.

References

[1] Wilson, I., and Hafner, F., "Benefit Assessment of Using Continuous Descent Approaches at Atlanta," *The 24th Digital Avionics Systems Conference Proceedings*, Vol. 1, Inst. of Electrical and Electronics Engineers, Washington, D.C., 2005, pp. 2.B.2–2.1-7.doi:10.1109/DASC.2005.1563318

[2] Dinges, E., "Determining the Environmental Benefit of Implementing Continuous Descent Approach Procedures," USA/Europe Air Traffic Management Research and Development Seminars, EUROCONTROL Paper 17, July 2007.

[3] Coppenbarger, R. A., Mead, R. W., and Sweet, D. N., "Field Evaluation of the Tailored Arrivals Concept for Datalink-Enabled Continuous Descent Approaches," AIAA Paper 2007-7778, 2007.

[4] Wubben, F. J. M., and Bussink, J. J., "Environmental Benefits of Continuous Descent Approaches at Schiphol Airport Compared with Conventional Approach Procedures," National Aerospace Lab., TR NLR-TP-2000-275, Amsterdam, May 2000.

[5] Tan Ho, N., and Clarke, J.-P. B., "Mitigating Operational Aircraft Noise Impact by Leveraging on Automation Capability," AIAA Paper 2001-5239, 2001.

[6] Ren, L., Clarke, J.-P. B., and Tan Ho, N., "Achieving Low Approach Noise Without Sacrificing Capacity," *Proceedings of the 22nd Digital Avionics Systems Conference*, Vol. 1, Inst. of Electrical and Electronics Engineers, Piscataway, NJ, 2003, pp 1.E.3–1.1-9. doi:10.1109/DASC.2003.1245810

[7] Abbott, T. S., "Speed Control Law for Precision Terminal Area In-Trail Self Spacing," NASA Langley Research Center NASA/TM-2002-211742, Hampton, VA, July 2002.

[8] Ren, L., and Clarke, J.-P. B., "Flight-Test Evaluation of the Tool for Analysis of Separation and Throughput," *Journal of Aircraft*, Vol. 45, No. 1, Jan.–Feb. 2008, pp. 323–332. doi:10.2514/1.30198

[9] de Gaay Fortman, W. F. M., van Paassen, M. M., Mulder, M., In 't Veld, A. C., and Clarke, J.-P. B., "Implementing Time-Based Spacing for Decelerating Approaches," *Journal of Aircraft*, Vol. 44, No. 1, Jan.–Feb. 2007, pp. 106–118. doi:10.2514/1.22253

[10] de Prins, J. L., Schippers, K. F. M., Mulder, M., van Paassen, M. M., In 't Veld, A. C., and Clarke, J.-P. B., "Enhanced Self-Spacing Algorithm for Three-Degree Decelerating Approaches," *Journal of Guidance, Control, and Dynamics*, Vol. 30, No. 2, Mar–Apr 2007, pp. 576–590. doi:10.2514/1.24542

[11] In 't Veld, A. C., van Paassen, M. M., Mulder, M., and Clarke, J.-P. B., "Pilot Support for Self-Separation during Decelerating Approaches," AIAA Paper 2004-5102, 2004.

[12] de Beer, B. A. F., Mulder, M., van Paassen, M. M., and In't Veld, A. C., "Development of an Ecological Interface for the Three-Degree Decelerating Approach," AIAA Paper 2008-7108, 2008.

[13] Clarke, J.-P. B., "A Systems Analysis Methodology for Developing Single Event Noise Abatement Procedures," Ph.D. Dissertation,

Massachusetts Inst. of Technology, Cambridge, MA, 1997.

[14] Slater, G. L., "Dynamics of Self-Spacing in a Stream of In-Trail Aircraft," AIAA Paper 2002-4927, 2002.

[15] Vilaplana, M. A., Gallo, E., Navarro, F. A., and Swierstra, S., "Towards A Formal Language for the Common Description of Aircraft Intent," *The 24th Digital Avionics Systems Conference Proceedings*, Inst. of Electrical and Electronics Engineers, Vol. 1, Washington, D.C., 2005, pp. 3.C.5–3.1-9.
doi:10.1109/DASC.2005.1563351

[16] de Leege, A. M. P., *Three-Degree Decelerating Approaches in Arrival Streams*, M.Sc. Thesis, Delft Univ. of Technology, Delft, The Netherlands, Sept. 2007.

[17] BAA Heathrow Flight Evaluation Report 2007," British Airports Authority, 2007, http://www.baa.com/assets//B2CPortal/Static%20Files/Noise%20Booklet.pdf [retrieved 31 Jan. 2009].

[18] *London BAA Gatwick Flight Evaluation Report 2006/07*, British Airports Authority, 2007, http://www.baa.com/assets/B2CPortal/Static%20Files/FEU%20Report%202006-07.pdf [retrieved 31 Jan. 2009].